RSC Advances

ROYAL SOCIETY OF CHEMISTRY

www.rsc.org/advances

Title

Effect of Heat Treatment Time to Cycle Performance of $LiMn_2O_4$ with "Nano Inclusion" for Lithium Ion Battery

Author

Shogo Esaki[1,2], Motoaki Nishijima[2], Shigeomi Takai[1], and Takeshi Yao[3,4,*]

Affiliation

1 Department of fundamental energy science, Graduate School of Energy Science, Kyoto University,

2 Materials and Energy Technology Laboratories, Corporate Research and Development Group, SHARP CORPORATION,

3 Kagawa National College of Technology

4 Institute of Advanced Energy, Kyoto University

Address

1 Yoshida, Sakyo-ku, Kyoto 606-8501, Japan

2 2613-1, Ichinomoto-cho, Tenri, Nara 632-8567, Japan

3 335 Chokushi-cho, Takamatsu, Kagawa 761-8058, Japan

4 Gokasho, Uji, Kyoto 611-0011, Japan

* Corresponding author

t_yao@hera.eonet.ne.jp

Abstract

The $LiMn_2O_4$ cathode material with "Nano Inclusion" has been prepared by employing various heat treatment time. The effect of heat treatment time on the electrochemical properties has been investigated. XRD powder pattern analysis and SEM observation indicated that $LiMn_2O_4$ formed at the low temperature sintering collapsed at the initial stage of the heat treatment and $LiMn_2O_4$ particles with $ZnMn_2O_4$ "Nano Inclusion" grew in the subsequent heat treatment. HAADF-STEM images revealed that both the particle size of $LiMn_2O_4$ and that of "Nano Inclusion" increased as the heat treatment time increased. Whereas all the $LiMn_2O_4$ samples with "Nano Inclusion" exhibit decreased initial discharge capacity in comparison with $LiMn_2O_4$ without "Nano Inclusion", they show the improved discharge capacity retention rate. The heat-treated for 4 hours sample surpass $LiMn_2O_4$ without "Nano Inclusion" in discharge capacity at over the 31st cycle. The larger the size of "Nano Inclusion", the more the crack propagation was considered to be suppressed, on the other hand, the larger the dead region increase. It is considered that appropriate size of "Nano Inclusion" was formed by the 4 hours heat treatment.

Introduction

The spinel $LiMn_2O_4$ has attracted much attention as a cathode material of lithium ion battery because of nontoxicity, availability, low cost and safety. However, $LiMn_2O_4$ suffer a severe capacity fading during charge and discharge cycles. Many trials have been investigated for improving the cycle performance. Substitution of Mn with other element has been tried to restrain the phase transition and stabilize the crystal structure. [1-12] A surface modification of $LiMn_2O_4$ with other compounds has been attempted to protect Mn from dissolution. [13-17] Stabilizing $LiMn_2O_4$ spinel crystal lattice with another spinel crystal inert to electrochemical reaction thorough the common oxide ion arrangement has been presented. [18,19] On the other hand, one of the major reasons to degenerate the charge / discharge capacity was proposed to be crack formation as well as the resulting dead region caused by the volume changes in active electrode material during the electrochemical charge and discharge processes.[20-23]

We previously reported a novel approach to improve the cycle performance of $LiMn_2O_4$ by using "Nano Inclusion", [24,25] where plate shaped $ZnMn_2O_4$ crystals with spinel structure grow in the $LiMn_2O_4$ single crystal. The induction of "Nano Inclusion" within the $LiMn_2O_4$ single crystal attained excellent cycle performance with a little decreased discharge capacity. "Nano Inclusion" is considered to suppress crack formation and propagation caused by volume change during charge / discharge process, which prevent the formation of dead region in $LiMn_2O_4$ to lead to capacity

degeneration.

In this study, we prepared $LiMn_2O_4$ with "Nano Inclusion" by employing various heat treatment time and investigated the effect of heat treatment time to cycle performance of $LiMn_2O_4$ with "Nano Inclusion".

Experiment

Sample preparation. — Zinc oxide (> 99 %, Wako Pure Chemical Industries) and tin oxide (99.9 %, Japan Pure Chemicals) were mixed in a molar ratio of Zn: Sn = 2: 1. The mixture was fired at 1000 °C for 12 h and crushed by planetary ball mill (PULVERISETTE series 5, FRITSCH Corp. Ltd.). Thus obtained material was confirmed to be a single phase of Zn_2SnO_4 with spinel structure by X-ray diffraction (XRD) with Cu Kα radiation (RAD-C, Rigaku Corp. Ltd.). Lithium carbonate (99.9 %, Hayashi Pure Chemicals), manganese dioxide (96.28%, Tosoh) and above obtained Zn_2SnO_4 were mixed with a molar ratio of Li : Mn : Zn_2SnO_4 = 0.95 : 1.9 : 0.05. The mixture was calcinated at 550 °C for 12 h in air and then heat-treated at 800 °C for various heat treatment time z (z = 0, 0.5, 2, 4, 6, 8, 12) hours in air. The obtained samples were denoted as the value of z hereafter.

X-ray diffraction, scanning electron microscopy, and electron microscopy measurement. — Powder

XRD patterns of the synthesized samples were collected from 10 ° to 90 ° in the 2θ range at a rate 1 ° per min with 0.01 ° step width by using Cu Kα radiation to identify the products. The sample morphology was investigated by scanning electron microscopy (SEM, XL-30 FEG, Philips) at an accelerating voltage of 10 kV. To observe the cross section of the samples, thin specimens were embedded into silicone resin followed by Ga^+ focused ion beam thinning. Observation of the cross section for the samples was carried out by using high-angle annular dark-field scanning transmission electron microscopy (HAADF-STEM, HF-2210, Hitachi, Ltd. Japan) with EDX analytical attachment (Noran Voyager, Noran Instruments Inc.) at an accelerating voltage of 200 kV for observation and with the electron beam spot size 0.7 nm for EDX analysis.

Electrochemical measurement. —The cycle performance of the sample was investigated with a two-electrode cell. The obtained sample was mixed with acetylene black (Denkikagaku Kogyo) as a conducting additive and polyvinylidene difluoride (PVdF, Kishida Chemical Corp. Ltd.) as an adhesive agent in a weight ratio of 80 : 15 : 5. The mixture was spread on an aluminum foil by using *n*-methyl pyrrolidone as a solvent, dried at 150 °C in vacuum and punched into disks 16 mm in diameter, which were served as cathode electrode. Lithium metal foil was used as a counter electrode. A mixture of ethylene carbonate and dimethyl carbonate in a volume ratio of 2 : 1 with a 1 M solution of $LiPF_6$ (LBG-00938 LiPF6, EC/DMC, Kishida Chemical Corp. Ltd.) was used as the

electrolyte. The cell was assembled in a glove box under an argon atmosphere using the above materials. Cycle tests were carried out at 1 C rate in the voltage range 3.2 - 4.3 V (vs. Li/Li^+) at the constant temperature 25°C.

Results and discussion

The coating weights of the electrode were 4.05 – 4.32 mg/cm^2 and the electrode densities were 1.54 – 1.69 g/cm^3, almost similar for all samples. Figure 1 shows the charge / discharge curves of $LiMn_2O_4$ without "Nano Inclusion" and with "Nano Inclusion" for various heat treatment time. The weight in the capacity contains "Nano Inclusion" hereafter. The specific capacities for all the samples with "Nano Inclusion" are smaller than that of $LiMn_2O_4$ without "Nano Inclusion". Figure 2 shows discharge capacity as a function of cycle number for $LiMn_2O_4$ without "Nano Inclusion" and with "Nano Inclusion". Although the first discharge capacity for any of the samples with "Nano Inclusion" was lower than that of $LiMn_2O_4$ without "Nano Inclusion", capacity fading during the charge / discharge cycles is clearly suppressed. The discharge capacity retention rate after 100 cycles were 0.958, 0.995, 1.04, 0.981, 0.968, 0.992, and 0.862 for the samples of z = 0.5, 2, 4, 6, 8, 12 with "Nano Inclusion", and $LiMn_2O_4$ without "Nano Inclusion", respectively. The cycle performance changes according to the value of z. The sample of z = 4 indicated the good capacity retention rate

and even showed the higher discharge capacity than that of $LiMn_2O_4$ without "Nano Inclusion" at over the 31st cycles. To observe the effect of heat treatment condition, we plotted the first discharge capacity and discharge capacity retention rate against the heat treatment time *z* in Fig. 3. Figure 3 (a) indicates that the first discharge capacity increased with the increase of heat treatment time up to z = 4, then decreased with *z*. Figure 3 (b) indicates that the discharge capacity retention rate once increased up to z = 4 and thereafter it remained constant or a little decreased. Similar tendency was observed for both 50 and 100th cycles.

XRD patterns of the prepared samples after various heat treatment time are shown in Fig. 4. The XRD pattern for the sample of z = 0, which is the just calcined sample at 550 °C for 12 h, indicates that $LiMn_2O_4$ forms after the calcinations at 550 °C, while Zn_2SnO_4 remains and seems not to form $ZnMn_2O_4$. For the samples of $z \geq 0.5$, the obtained XRD patterns indicate the existence of SnO_2 and $ZnMn_2O_4$ as well as $LiMn_2O_4$. The crystallite size of $LiMn_2O_4$ was estimated from the Scherrer's equation,

$$L = \frac{K\lambda}{\beta \cos\theta} \qquad (1)$$

where *L*, *K*, λ, β, and θ are the average crystallite size, a constant related to crystallite shape, normally taken as 0.9, the X-ray wavelength in nanometer, the peak width of the diffraction peak profile at half maximum height, and the scattering angle, respectively. The crystallite size, *L,* is plotted against the value of *z* in Fig. 5. Figure 5 indicates the crystallite size decreases at first from *z*

= 0 to z = 0.5, then increases with increasing the heat treatment time z. It is considered that the $LiMn_2O_4$ crystal once formed at the calcination process decomposes at the heat treatment process and that the collapsed $LiMn_2O_4$ crystal regrew with $ZnMn_2O_4$ "Nano Inclusion" during the prolonged heat treatment process.

SEM images of the samples are shown in Fig. 6. In Fig. 6 (a), crystal facet characteristic for cubic symmetry with the size of about 150 - 750 nm was observed. This means that the cubic spinel with high crystallinity has already been formed only by the heat treatment at 550 °C. The crystallite size decreased from $z = 0$ to $z = 0.5$ as indicated in Fig. 5. The crystal facet disappeared at $z = 0.5$ as Fig. 6 (b). This means that the collapse of $LiMn_2O_4$ crystal at the initial stage of the heat treatment was detected by the SEM observation. The particle size appears to increase with the increase of heat treatment time as observed in Fig. 6 (c) and (d). Such a crystal collapse and regrow behavior is consistent with the result of the XRD measurement.

HAADF-STEM cross section images of $LiMn_2O_4$ particles and the corresponding EDX element maps are shown in Fig. 7. The particles of $LiMn_2O_4$ were observed. For the sample of $z = 0$, it is observed that the Zn existence at Zn element map coincides with the Sn existence at Sn element map. It is considered that the area where the Zn existence corresponds to the Sn existence is Zn_2SnO_4 by taking the XRD results into consideration. "Nano Inclusion", which consists of Zn and Mn, is $ZnMn_2O_4$ as described in our previous study. [24,25] For the sample of $z = 0.5$, 4, and 12, it is

observed that white lines with about few tens of nanometer as indicated by arrows at each HAADF-STEM image coincide with the Zn line at each Zn element map. Both gray areas and white lines coincide with the Mn existence at each Mn element map. It is indicated that white lines are $ZnMn_2O_4$ by taking the XRD results into consideration. These white lines correspond to "Nano Inclusions". Whereas "Nano Inclusion" was not detected at all in the sample of $z = 0$, they were observed in the sample of $z = 0.5$, 4, and 12. HAADF-STEM images also revealed that the particle size of $LiMn_2O_4$ increased as z increased. Taking all the results into consideration, it is indicated that $LiMn_2O_4$ crystals grew during the heat treatment process. As shown in Fig. 7 (b), (c), and (d), the size of "Nano Inclusion" was 5 – 40 nm, 20 – 60 nm, and 20 – 250 nm, for the sample of $z = 0.5$, 4, and 12, respectively. "Nano Inclusion" grew at the process of heat treatment. As shown in Fig. 7 (d), "bright white particles" at HAADF image coincide with the Sn existence at Sn element map. It is obvious that these bright white particles are SnO_2 by taking the XRD results into consideration. It is indicated that SnO_2 is considered to be excluded from $LiMn_2O_4$ by taking the HAADF image into account. SnO_2 is nonreactive to charge and discharge reaction in the voltage range of this study. SnO_2 is just an impurity in the system of $LiMn_2O_4$ with "Nano Inclusion".

It is reported that active electrode materials change their dimensions during the charge and discharge process, resulting in the crack formation, and crack propagation which induce the dead region to lead to the capacity fading.[20-23] "Nano Inclusion", nonreactive to charge and discharge

reaction, is considered to suppress crack propagation and then prevent capacity fading. With the increase of "Nano Inclusion" size, the effect for suppression of the crack formation and propagation is considered to increase. This results in good cycle performance. When surrounded by "Nano Inclusions", the region which has no electrical contact with environment is generated. Then this region does not contribute to electrochemical reaction, even though the material has no degradation. This non-electrochemical active region is the dead region. On the other hand, the dead region of $LiMn_2O_4$ for the electrochemical reaction is considered to increase. This results in a reduction of discharge capacity. In the system of $LiMn_2O_4$ with "Nano Inclusion", the size of "Nano Inclusion" and $LiMn_2O_4$ increase with the increase of heat treatment time. The larger the particle size of $LiMn_2O_4$, the higher the capacity. When the heat treatment time is short, the size of "Nano Inclusion" and $LiMn_2O_4$ is relatively small. The effect for suppression of the crack formation and propagation is low and the discharge capacity is low. This results in poor cycle performance and low discharge capacity. As the heat treatment time increases, both the sizes of $LiMn_2O_4$ particle and that of "Nano Inclusion" increase, the cycle performance increases, and the discharge capacity increases. For the long heat treatment time, the size of "Nano Inclusion" become too large. The cycle performance is better but the capacity is suppressed by the large "Nano Inclusion" due to the increase of the dead region of $LiMn_2O_4$ for the electrochemical reaction. In the system of $LiMn_2O_4$ with "Nano Inclusion", a proper size of $LiMn_2O_4$ and "Nano Inclusion" is considered to achieve higher capacity

with better cycle performance. The proper size of "Nano Inclusion" results in suppressing crack formation and propagation with making the dead region of $LiMn_2O_4$ for the electrochemical reaction smaller.

Conclusions

We fabricated $ZnMn_2O_4$ "Nano Inclusion"-induced $LiMn_2O_4$ cathode material by employing various heat treatment time to investigate the effect of heat treatment time to cycle performance of $LiMn_2O_4$ with "Nano Inclusion". For the capacity retention rate, all the samples with "Nano Inclusion" were larger than $LiMn_2O_4$ without it. Discharge capacity of the sample heat-treated for 4 h surpassed that of $LiMn_2O_4$ at more than 31st cycle. It is considered that appropriate size of "Nano Inclusion" was formed by the 4 h heat treatment.

References

1. L. Guohua, H. Ikuta, T. Uchida and M. Wakihara, *J. Electrochem. Soc.*, **143**, 178 (1996).

2. H. J. Choi, K. M. Lee and J. G. Lee, *J. Power Sources*, **103**, 154 (2001).

3. C.H. Shen, R.S. Liu, R. Gundakaram, J.M. Chen, S.M. Huang, J.S. Chen and C.M. Wang, *J.*

Power Sources, **102**, 21 (2001).

4. C. Sigala, D. Guyomard, A. Verbaere, Y. Piffard and M. Tournoux, *Solid State Ionics*, **81**, 167 (1995).

5. A. D. Robertson, S. H. Lu and W. F. Howard, Jr., *J. Electrochem. Soc.*, **144**, 3505 (1997).

6. A. D. Robertson, S. H. Lu, W. F. Averill and W. F. Howard, Jr., *J. Electrochem. Soc.*, **144**, 3500 (1997).

7. Y. Xia and M. Yoshio, *J. Electrochem. Soc.*, **143**, 825 (1996).

8. Y. Gao and J. R. Dahn, *J. Electrochem. Soc.,* **143**, 100 (1996).

9. J. M. Tarascon, E. Wang, F. K. Shokoohi, W, R. McKinnon and S. Colson, *J. Electrochem. Soc.*, **138**, 2859 (1991).

10. A. de Kock, E. Ferg and R.J. Gummow, *J. Power Sources*, **70**, 247 (1998).

11. F. Le Cras, D. Bloch, M. Anne and P. Strobel, *Solid State Ionics*, **89**, 203 (1996).

12. R.J. Gummow, A. de Kock and M.M. Thackeray, *Solid State Ionics*, **69**, 59 (1994).

13. S. Guo, X. He, W. Pu, Q. Zeng, C. Jiang and C.Wan, *Int. J. Electrochem. Sci.*, **1**, 189 (2006).

14. Y.-K. Sun, K.-J. Hong and J.Prakash, *J. Electrochem. Soc.*, **150**, A970 (2003).

15. S.-W. Lee, K.-S. Kima, H.-S. Moon, H.-J. Kim, B.-W. Cho, W.-I. Cho, J.-B. Ju and J.-W. Park, *J. Power Sources*, **126**, 150 (2004).

16. A. Eftekhari, *Solid State Ionics*, **167**, 237 (2004).

17. G.G. Amatucci, A. Blyr, C. Sigala, P. Alfonse and J.M. Tarascon, *Solid State Ionics*, **104**, 13 (1997).

18. N. Ozawa, K. Donoue and T. Yao, *Electrochem. Solid-State Lett.*, **6**, A106 (2003).

19. M. Hibino, M. Nakamura, Y. Kamitaka, N. Ozawa and T. Yao, *Solid State Ionics*, **177**, 2653 (2006).

20. H. Wang, Y.-I. Jang, B. Huang, D. R. Sadoway and Y.-M. Chiang, *J. Electrochem. Soc.*, **146**, 473 (1999).

21. Toray Research Center, Inc. Japan, TRC poster sessions 2003 VII-1, "Crystal Analysis for Cathode Materials of Lithium Ion Batteries", Tokyo, (2003).

22. D. Wang, X. Wu, Z. Wang and L. Chen, *J. Power Sources*, **140**, 125 (2005).

23. H. Gabrisch, J. Wilcox and M. M. Doeff, *Electrochem. Solid-State Lett.*, **11**, A25 (2008).

24. S. Esaki, M. Nishijima and T. Yao, *ECS Electrochem. Lett.*, **2**, A93 (2013).

25. S. Esaki, M. Nishijima, S. Takai and T. Yao, *RCS Adv.*, **4**, 59858 (2014).

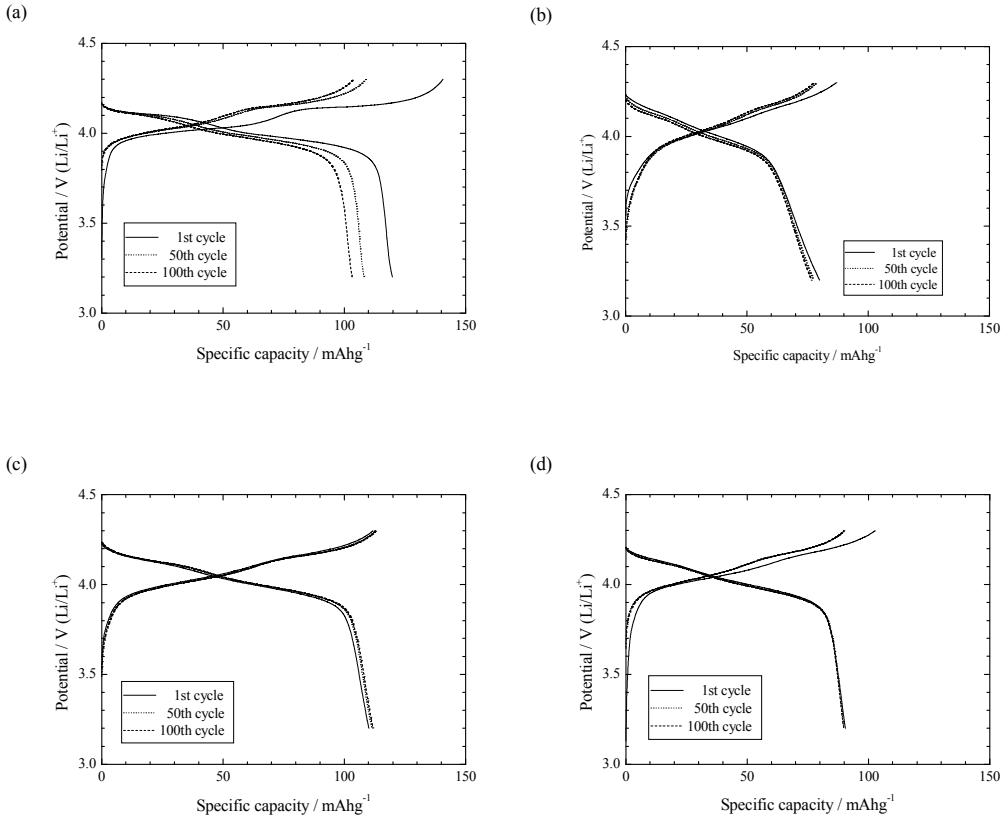

Figure 1 The charge / discharge curves of the samples: (a) $LiMn_2O_4$ without "Nano Inclusion", (b) z = 0.5, (c) z = 4, (d) z = 12. The weight in the capacity contains "Nano Inclusion"

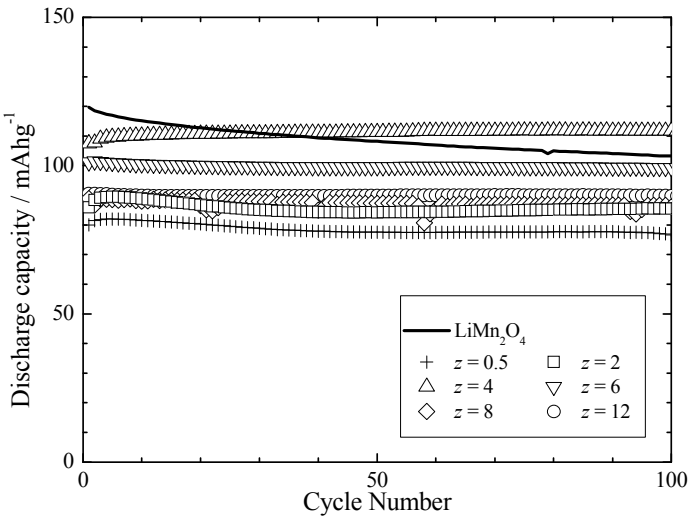

Figure 2 Discharge capacity against cycle number. The weight in the capacity contains "Nano Inclusion"

(a)

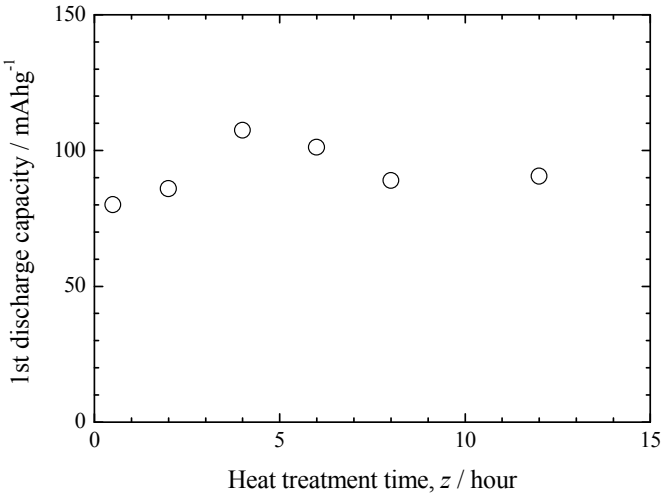

(b)

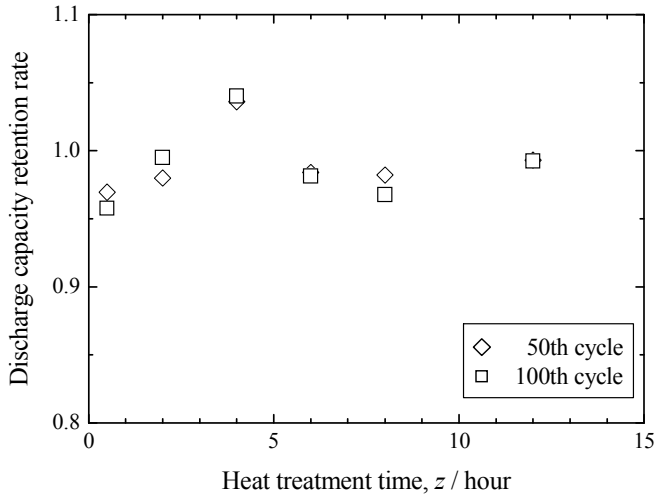

Figure 3 Discharge performance against heat treatment time *z*: (a) 1st discharge capacity, (b) discharge capacity retention rate. The weight in the capacity contains "Nano Inclusion"

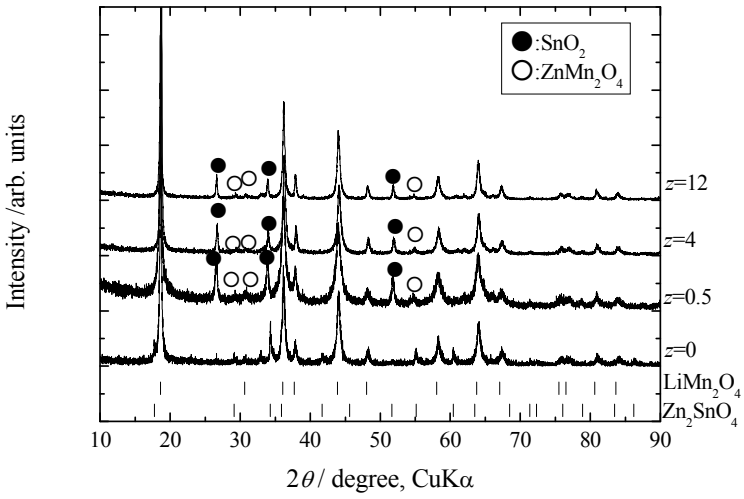

Figure 4 XRD patters of the samples. The vertical lines indicate the positions calculated from Bragg reflection for $LiMn_2O_4$ and Zn_2SnO_4. SnO_2 and $ZnMn_2O_4$ are indicated by a filled circle and an open circle, respectively.

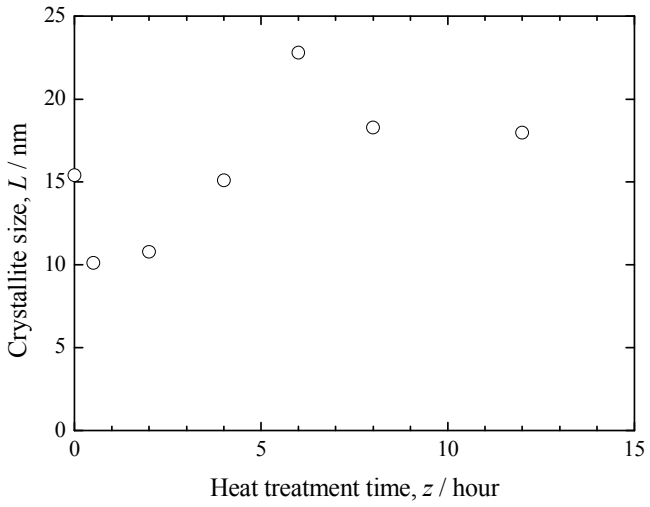

Figure 5 Crystallite size, L, against the heat treatment time, z.

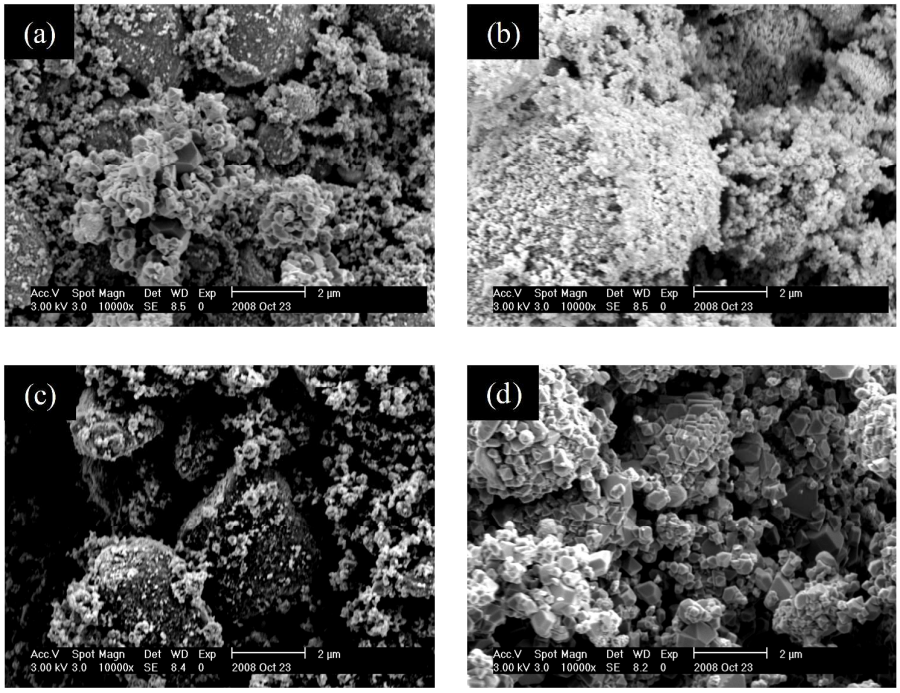

Figure 6 SEM images of the samples: (a) $z = 0$, (b) $z = 0.5$, (c) $z = 4$, (d) $z = 12$.

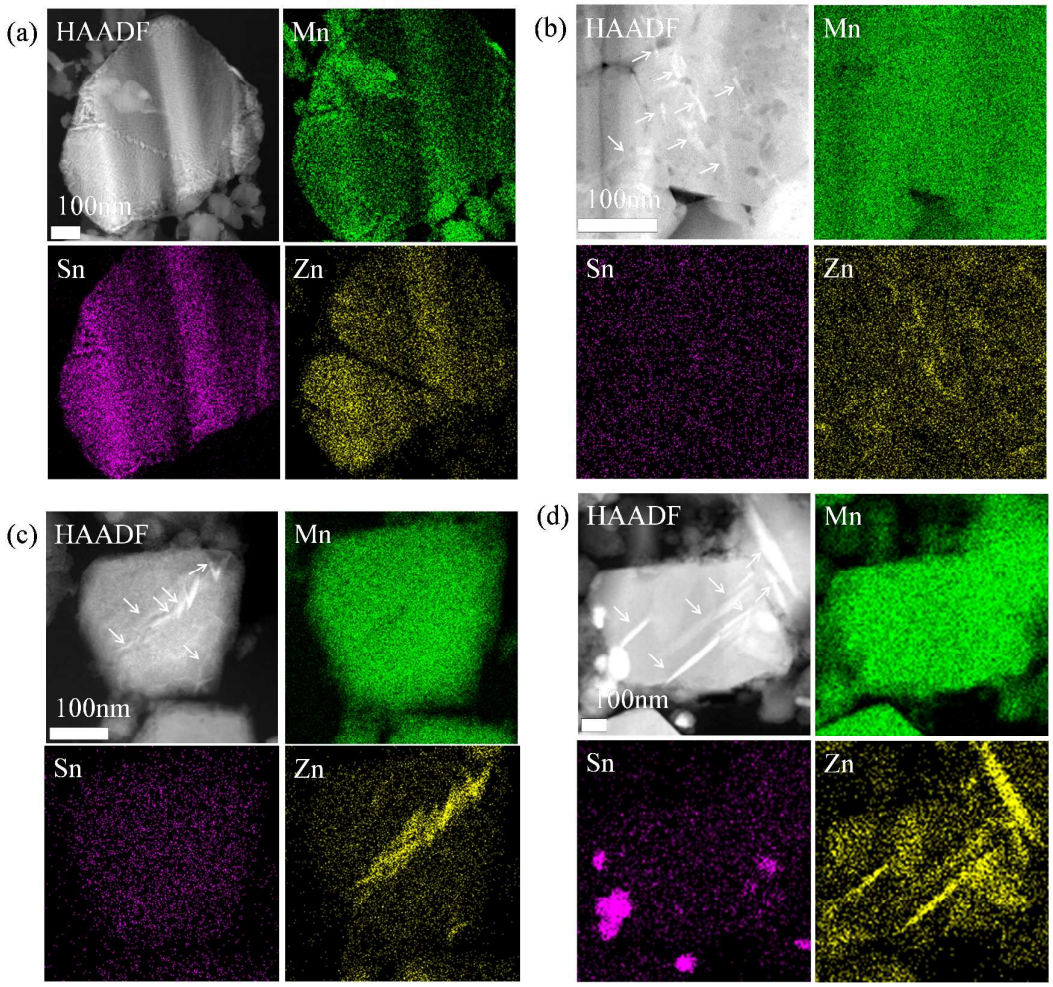

Figure 7 HAADF-STEM images and EDX element maps for the samples: (a) $z = 0$, (b) $z = 0.5$, (c) z = 4, (d) $z = 12$. Green, violet, and yellow indicate Mn, Sn, and Zn, respectively.